Effect of N/Z in pre-scission neutron multiplicity for ^{16,18}O + ^{194,198}Pt systems

Rohit Sandal,[*] B. R. Behera,[†] Varinderjit Singh, Maninder Kaur, A. Kumar, G. Singh, and K. P. Singh
Department of Physics, Panjab University, Chandigarh 160014, India

P. Sugathan, A. Jhingan, K. S. Golda, M. B. Chatterjee, and R. K. Bhowmik[‡]
Inter University Accelerator Centre, Aruna Asaf Ali Marg, New Delhi 110067, India

Sunil Kalkal,[§] D. Siwal, S. Goyal, and S. Mandal
Department of Physics and Astrophysics, University of Delhi, New Delhi 110007, India

E. Prasad[‖]
Department of Physics, Calicut University, Calicut 673635, India

K. Mahata and A. Saxena
Nuclear Physics Division, Bhabha Atomic Research Centre, Mumbai 400085, India

Jhilam Sadhukhan[¶]
Department of Physics and Astronomy, University of Tennessee, Knoxville, Tennessee 37996, USA and Physics Division, Oak Ridge National Laboratory, Oak Ridge, Tennessee 37831, USA

Santanu Pal
Physics Group, Variable Energy Cyclotron Centre, 1/AF Bidhan Nagar, Kolkata 700064, India
(Received 13 September 2012; published 9 January 2013)

Pre-scission neutron multiplicities from fission of the compound nuclei ^{210,212,214,216}Rn have been measured in order to investigate the N/Z dependence of fission hindrance. The Rn isotopes are populated through the fusion of ^{16,18}O + ^{194,198}Pt systems and are formed at four excitation energies in the range of 50–79 MeV. The experimental pre-scission neutron yield is compared with predictions from the statistical model of compound nuclear decay containing the strength of nuclear dissipation as a free parameter. The strength of nuclear dissipation obtained in the present analysis does not show any specific dependence on the N/Z values of the fissioning nuclei at large excitation energies. The dissipation strength at the lowest excitation energy, however, indicates a shell closure effect at $N = 126$ for the ^{212}Rn isotope.

DOI: 10.1103/PhysRevC.87.014604 PACS number(s): 25.70.Jj, 25.70.Gh, 24.10.Pa

I. INTRODUCTION

It is now well established that the pre-scission neutron multiplicity is one of the most efficient probes to study the fission time scale in heavy ion induced fusion-fission reactions [1]. This has been possible due to the fact that the neutrons emitted from a compound nucleus before fission are kinemetically well separated from the neutrons emitted from the fission fragments, and hence their multiplicity can be accurately measured. It has been observed that the experimental multiplicities of pre-scission neutrons were in clear excess of the predictions of the standard statistical model of compound nuclear decay [1,2]. Similar observations were also made for pre-scission light charged particles [3] and GDR gamma rays [4]. The excess in multiplicities indicates the presence of a dynamic hindrance of the fission process, and careful analyses of pre-scission multiplicities of light particles and γ [5–8] and evaporation residue cross-sections [9,10] have shown that the fission dynamics of an excited compound nucleus is dissipative in nature at high excitation energies.

The number of neutrons (or any other evaporated particle) emitted prior to scission in a fission event is affected by the dissipation in fission dynamics in three significant ways. First, as was shown by Kramers [11], dissipation increases the fission lifetime relative to that obtained from the standard Bohr-Wheeler statistical model [12], which arises because fission is a quasistationary diffusion process [13–16] over the barrier. Second, an additional time interval is available for neutron emission during the transient time required by the system to build up the quasistationary probability flow over the barrier. This time interval is also determined by the strength of the dissipation [14]. Third, still more neutrons can be emitted during the time interval during which the system descends

[*]Present address: S. V. Government College Ghumarwin, Bilaspur 174021 (H.P.), India.
[†]Corresponding author: bivash@pu.ac.in
[‡]Present address: Guru Ghasi Das University Bilaspur 495009 (C.G.), India.
[§]Present address: Indiana University, South Bend, Indiana 46615, USA.
[‖]Present address: Department of Physics, Central University of Kerala, Kasaragod 671314, India.
[¶]On leave of absence from VECC, Kolkata 700064, India.

from the saddle point to the scission, which is increased by the dissipation [17].

The above dynamical effects on fission probability have been exploited in the past for studying the nature of nuclear viscosity. For instance, calculations of the lifetimes of the excess pre-scission neutrons have been used to estimate the fission delay time [6,18], which depends directly on the magnitude of the viscosity. In order to obtain the information on the dissipation strength beyond the saddle point, i.e., the saddle-to-scission dissipation strength, it is necessary to employ those observables which can be affected by the saddle-to-scission dissipation effects. Several of such studies involved measurements of particle multiplicities at various excitation energies, at different entrance channel mass asymmetries [19,20] and as a function of fissility [18] of the compound nucleus.

The problem of the origin and the nature of nuclear dissipation is presently one of the most interesting questions in nuclear physics at low and intermediate energies. Dissipation in mean-field nuclear dynamics accounts for the coupling of the collective motion with the particle degrees of freedom. The single-particle energy spectra has a well defined shell structure which persists at least at low nuclear excitations [21]. It is therefore of considerable interest to explore the effect of increasing N/Z in compound nuclei for a given element on the strength of nuclear dissipation. Measurement of pre-scission neutron multiplicities from an isotopic chain will be a suitable tool for the above purpose.

Pre-scission neutron multiplicities from compound nuclei with the same Z but different N have been measured earlier [22–24]. The N/Z dependence of the sensitivity of the neutron multiplicity with respect to the dissipation strength has also been theoretically investigated [25,26]. However, the experimental studies of Refs. [22,23] considered very different entrance channels to populate the compound nuclei at different excitation energies. Pre-scission neutron multiplicities were measured for three Fr isotopes (^{213,215,217}Fr) in Ref. [24]. In order to investigate the N/Z dependence over a wider isotopic range, we report here experimental measurement of pre-scission neutron multiplicities from four compound nuclei, namely ^{210,212,214,216}Rn, and statistical model analysis of the data. The compound nuclei ^{210,212,214,216}Rn having N/Z values as 1.441, 1.465, 1.488, 1.511 respectively are populated through the ^{16,18}O + ^{194,198}Pt reactions at a different set of excitation energies in the present work.

The paper is organized as follows. The experimental details are given in the next section. Section III contains the data analysis and the experimental results. The statistical model analysis is described in Sec. IV followed by a summary and the conclusions in the last section.

II. EXPERIMENTAL PROCEDURE

The measurements were carried out at 15UD Pelletron + First Module of the Super Conducting Linear accelerator (LINAC) and National Array of Neutron Detectors (NAND) facility at Beam Hall-II of the Inter University Accelerator Centre (IUAC), New Delhi. Pulsed beams ^{16}O and ^{18}O were

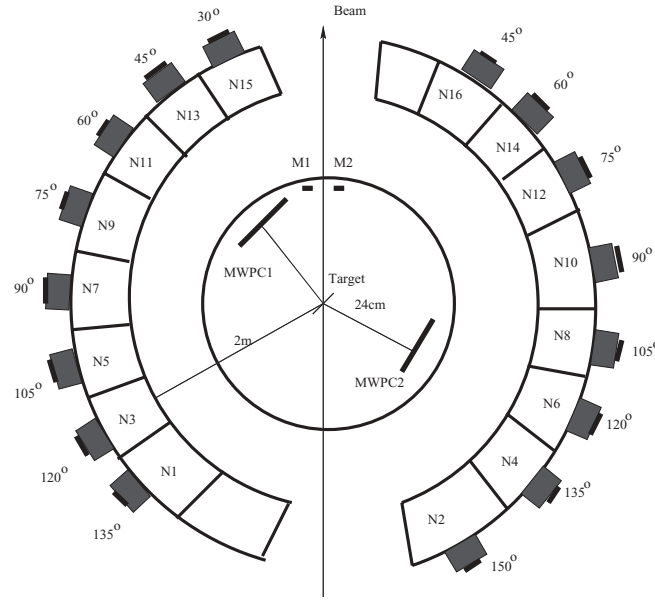

FIG. 1. Experimental setup in NAND at IUAC.

bombarded on ^{194}Pt and ^{198}Pt targets to populate the compound nuclei ^{210,212,214,216}Rn at excitation energies of 50, 61, 71.7, and 79 MeV. The ^{194}Pt target was either a 1.75 mg/cm^2 rolled platinum metal foil or a 530 μg/cm^2 thin layer of platinum deposited on a 15 μg/cm^2 thin carbon foil. The ^{198}Pt target was a rolled metal foil of thickness 1.45 mg/cm^2. Fission fragments were detected by a pair of large area multiwire proportional counters (MWPCs) (12.7 cm × 7.62 cm) kept at the fission fragment folding angle at distances of 18.5 and 17.0 cm from the target position. Two silicon surface barrier detectors were also placed at $\pm 16^o$ out of plane for normalization purpose inside the spherical scattering chamber of 60 cm diameter. The fast timing signal from the MWPCs were used to get the time-of-flight (TOF) information of the fission fragments with reference to the the beam arrival time, which enabled us to separate the fission events from other competing channels. Sixteen neutron detectors (BC501) were placed 2 m away from the target in a cylindrical fashion (Fig. 1) at different angles around the target chamber for the neutron TOF measurements.

In order to reduce the γ background, the beam dump was placed 4 m downstream from the target and the beam line was shielded with paraffin and lead bricks. The time spread in the beam was continuously monitored using a BaF_2 detector placed close to the beam dump, and it was found to be 600 ps at different beam energies. Discrimination between neutrons and γ rays was made by using the pulse shape analysis based on the zero crossing [27] and TOF technique. The TOF of neutrons were converted into neutron energy by considering the prompt peak of γ in the TOF spectrum for reference time. Data was also taken with a thick sheet of iron in front of a neutron detector to estimate the level of background in the neutron spectra; it was found to be negligible.

The recorded neutron energy distribution was corrected for the energy dependent efficiency of each detector. The efficiency curve of the neutron detector as a function of neutron energy was obtained by using the Monte Carlo computer code

MODEFF [28]. The Monte Carlo calculations, in turn, were verified by measuring the relative efficiency of the detector by using a ^{252}Cf spontaneous fission source. The threshold of the neutron detectors was kept at about 0.5 MeV by calibrating it with the standard γ sources (^{137}Cs and ^{60}Co) [29]. The trigger of the data acquisition was generated by logical OR of the two fission fragments (cathode of the two MWPCs) which was further AND-gated with the RF of the beam.

III. DATA ANALYSIS AND RESULTS

The pre- and post-scission components of neutron multiplicities are obtained from the measured neutron energy spectra by using a multiple source least-square fitting procedure, using the Watt expression [18,30]. Three moving sources of neutrons (the compound nucleus plus two fully accelerated fission fragments) are considered while determining the multiplicities from the simultaneous fits. The neutrons emitted from these moving sources are assumed to be isotropic in their respective rest frames. Thus the measured neutron multiplicities are given as

$$\frac{d^2M_n}{dE_n d\Omega_n} = \sum_{i=1}^{3} \frac{M_n^i \sqrt{E_n}}{2(\pi T^i)^{3/2}} \times \exp\left[-\frac{E_n - 2\sqrt{E_n E^i/A^i}\cos\theta^i + E^i/A^i}{T^i}\right]. \quad (1)$$

In the above, E_n is the neutron energy in the laboratory frame and A^i, E^i, T^i, and M_n^i are the mass, energy, temperature, and multiplicity of each neutron emitting source i. θ^i is the direction of a neutron with respect to the respective source. Fission fragment velocities and folding angles are obtained from the Viola [31] systematic for symmetric fission. The pre- and post-scission neutron multiplicities and temperatures denoted by $M^{\rm pre}$, $M^{\rm post}$, $T^{\rm pre}$, and $T^{\rm post}$ respectively (here $M^{\rm post}$ refers to the neutron multiplicity from one of the fragments) are determined from the least-square fits considering them as free parameters. The post-scission emission parameters $M^{\rm post}$ and $T^{\rm post}$ are considered to be same for both the fission-fragments. Minimum values of χ^2/(degrees of freedom) on the fitting procedure are in the range of 0.7 to 1.0. The errors shown are obtained from the fits and arise from statistical uncertainties. Fits are also obtained using $T^{\rm pre}$ as a fixed parameter as $T = \sqrt{(E^*/a)}$, where E^* is the excitation energy and a is the level density parameter, taken as $A/10$ for the compound nucleus (CN) where A is the mass number of the CN. $T^{\rm pre}$ is scaled down by a factor of 11/12 to account for multistep evaporation [32]. However, the neutron multiplicities thus obtained are found to be close to those obtained by keeping $T^{\rm pre}$ as a free parameter and are within the error bars.

The total average neutron multiplicity $M^{\rm tot}$ is obtained from the fitted values of $M^{\rm pre}$ and $M^{\rm post}$ as $M^{\rm tot} = M^{\rm pre} + 2M^{\rm post}$. All the multiplicities for all the systems are given in Table I.

The angular acceptance of both the neutron detectors and the fission detectors are taken into account while calculating the relative angle between the neutron and the source direction in the fitting procedure. Figure 2 shows the fits to the double differential neutron multiplicity spectra at various angles for ^{16}O + ^{194}Pt at 100 MeV of beam energy.

We next plot the pre-scission neutron multiplicities at each compound nuclear excitation energy as a function of N/Z in Fig. 3. While $M^{\rm pre}$ increases with N/Z at the three higher excitation energies, a minimum is observed for ^{212}Rn at the lowest excitation energy. Since the numbers of neutrons in the ^{210,212,214,216}Rn nuclei are 124, 126, 128, and 130 respectively, one might expect that the appearance of the above minimum is due to the shell closure effects at $N = 126$ for ^{212}Rn. If we assume $M^{\rm pre}$ is simply proportional to the neutron decay width, which in turn is approximately proportional to $\exp(-B_n/T)$, and use the experimental nuclear masses to obtain the last neutron binding energies (B_n) of ^{210,212,214,216}Rn as 8.74, 7.98, 6.69, and 6.65 MeV respectively, a monotonic increase of $M^{\rm pre}$ with N/Z is predicted. The trend remains the same when emission of the second neutron is also considered. Though the experimental $M^{\rm pre}$ values at the higher excitation energies agree with prediction, the appearance of the minimum at the lowest excitation energy remains to be explained. We therefore perform statistical model calculations in order to study the detailed nature of the experimental data.

IV. STATISTICAL MODEL ANALYSIS

In the statistical model calculation, emission of light particles (neutron, proton, and α) and giant dipole resonance (GDR) γ rays are considered as decay channels for an excited compound nucleus in addition to fission. The light particle and the GDR γ partial widths are obtained from the Weisskopf formula [33]. The fission width is calculated following the work of Kramers [11] where the dynamics of the fission degree of freedom is considered similar to that of a Brownian particle in a heat bath. The temperature of the heat bath which represents all the other nuclear degrees of freedom is given by the compound nuclear temperature T. The driving force in a thermodynamical system such as a hot nucleus is provided by the free energy of the system [34,35]. The free energy F is given by the Fermi gas model as

$$F(\mathbf{q}, T) = V(\mathbf{q}) - a(\mathbf{q})T^2, \quad (2)$$

where $\mathbf{q}$ represents the collective coordinates and the collective potential $V(\mathbf{q})$ is obtained from the finite-range liquid drop model (FRLDM) [36]. The rotational energy of the compound nucleus is obtained using the shape-dependent rigid body moment of inertia and is included in the FRLDM potential. In the above equation, $a(\mathbf{q})$ is the level density parameter which depends on the shape of the compound nucleus specified by the collective coordinates $\mathbf{q}$. Denoting the fission barrier in the free energy profile by F_B, the Kramers' fission width is given as [11,37],

$$\Gamma_K = \frac{\hbar\omega_g}{2\pi}\exp\left(\frac{-F_B}{T}\right)\left(\sqrt{1+\left(\frac{\beta}{2\omega_s}\right)^2} - \frac{\beta}{2\omega_s}\right), \quad (3)$$

where β is the dissipation coefficient. In the above equation, ω_g and ω_s are the harmonic oscillator potentials which have

TABLE I. Experimentally measured neutron multiplicities and temperatures for ^{16,18}O + ^{194,198}Pt reactions

Reactions	CN	N/Z	$E^{\rm lab}$ (MeV)[a]	E^* (MeV)	$M^{\rm pre}$ (±err)	$M^{\rm post}$ (±err)	$M^{\rm tot}$ (±err)	$T^{\rm pre}$ (±err)	$T^{\rm post}$ (±err)
^{16}O + ^{194}Pt	^{210}Rn	1.441	86.5	50	1.854 (0.07)	0.76 (0.03)	3.374 (0.10)	1.12 (0.03)	0.91 (0.02)
			98.4	61	2.37 (0.09)	0.88 (0.03)	4.13 (0.11)	1.23 (0.03)	1.00 (0.025)
			109.9[b]	71.7	2.77 (0.1)	0.89 (0.05)	4.55 (0.14)	1.52 (0.05)	1.002 (0.05)
			117.8[b]	79	3.24 (0.1)	0.832 (0.05)	4.904 (0.14)	1.49 (0.06)	1.00 (0.068)
^{18}O + ^{194}Pt	^{212}Rn	1.465	84.05	50	1.61 (0.07)	0.632 (0.02)	2.878 (0.10)	1.18 (0.03)	0.9 (0.02)
			96.1	61	2.53 (0.09)	0.806 (0.03)	4.142 (0.11)	1.19 (0.03)	0.90 (0.03)
			107.75[b]	71.7	2.95 (0.1)	0.722 (0.05)	4.39 (0.14)	1.47 (0.06)	1.00 (0.07)
			115.7[b]	79	3.32 (0.1)	0.859 (0.05)	5.038 (0.14)	1.49 (0.05)	1.001 (0.06)
^{16}O + ^{198}Pt	^{214}Rn	1.488	86.9	50	1.95 (0.08)	0.74 (0.02)	3.43 (0.10)	1.14 (0.03)	0.85 (0.023)
			98.75	61	2.76 (0.09)	0.78 (0.03)	4.32 (0.11)	1.16 (0.02)	0.90 (0.02)
			110.25	71.7	3.41 (0.1)	0.75 (0.04)	4.91 (0.13)	1.46 (0.04)	0.90 (0.05)
			118.2	79	3.53 (0.1)	0.836 (0.05)	5.202 (0.14)	1.52 (0.04)	1.009 (0.058)
^{18}O + ^{198}Pt	^{216}Rn	1.511	88.3	50	2.1 (0.1)	0.73 (0.025)	3.56 (0.11)	1.13 (0.06)	0.88 (0.08)
			100.35	61	2.93 (0.11)	0.85 (0.03)	4.63 (0.12)	1.24 (0.03)	0.91 (0.028)
			111.9	71.7	3.70 (0.1)	0.802 (0.05)	5.303 (0.14)	1.45 (0.04)	0.93 (0.025)
			119.8	79	3.83 (0.1)	0.801 (0.05)	5.432 (0.14)	1.45 (0.04)	0.93 (0.05)

[a]Corrected for energy loss in the target.
[b]Measurements were made with a 530 μg/cm^2 platinum target.

the same curvatures as those of the free energy profile at the ground state and at the saddle configurations respectively.

The Kramers' fission width of Eq. (3) represents a stationary fission rate which is reached after an initial delay or the transient time. This is taken into account in the statistical model calculation by using the following parametrized form of the time-dependent fission width [38]:

$$\Gamma_f(t) = \Gamma_K[1 - \exp(-2.3t/\tau_f)], \tag{4}$$

where the transient time τ_f is given as

$$\tau_f = \frac{\beta}{2\omega_g^2} \ln\left(\frac{10F_B}{T}\right).$$

In the statistical model calculation, a compound nucleus is followed in time over small time steps and at each time step, the fate of the compound nucleus is decided by a Monte Carlo sampling using the particle, γ, and the fission widths [39]. In the event of a particle or γ emission, the residual nucleus is appropriately redefined and its excitation energy and angular momentum adjusted through another Monte Carlo sampling procedure. The process continues till either the compound nucleus undergoes fission or an evaporation residue is formed. According to the definition of the Kramers' fission width, a fission event corresponds to the crossing of the saddle point by the compound nucleus. Hence for a fission event, the compound nucleus can emit further neutrons (or other particles) during its journey from saddle to scission which contributes to the pre-scission multiplicity. The number of such neutrons are also calculated by using the saddle-to-scission time interval given as [17]

$$\tau_{ss} = \tau_{ss}^o(\sqrt{1+\gamma^2} + \gamma), \tag{5}$$

where τ_{ss}^o is the nondissipative saddle-to-scission time interval [40]. We have also calculated the multiplicity of neutrons emitted from the fission fragments ($M^{\rm post}$) assuming symmetric fission.

An important input to the statistical model calculation is the level density parameter. The level density parameter is taken

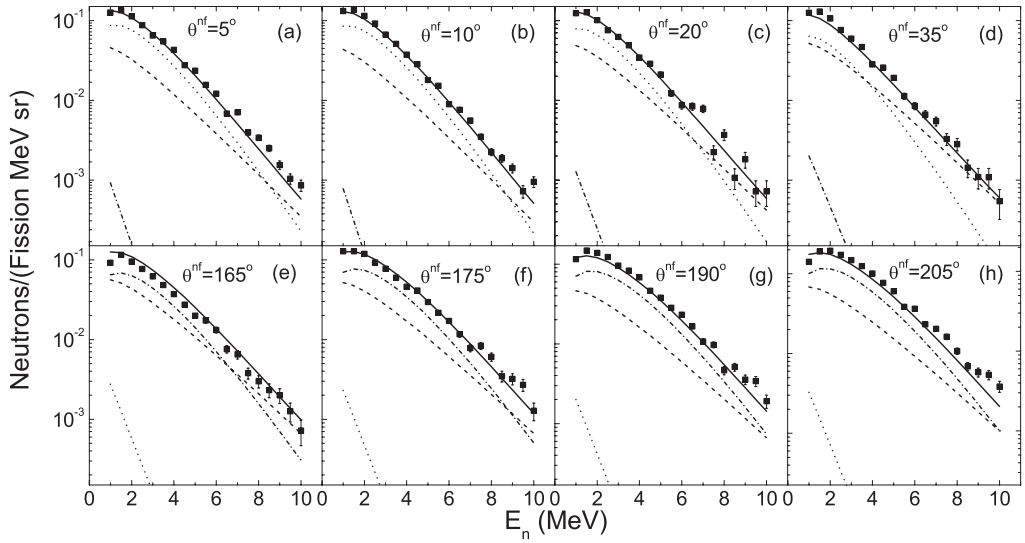

FIG. 2. (a)-(h) Double differential neutron energy spectra for $^{16}O + ^{194}Pt$ at 61 MeV excitation energy along with the fits for the pre-scission (dashed curve) and post-scission from one fragment (dotted curve) and that from the other (dot-dashed curve). The solid curve represents the total contribution.

from the work of Ignatyuk *et al.* [41] and is given as follows:

$$a(U) = \tilde{a}\left[1 + \frac{f(U)}{U}\delta W\right], \qquad f(U) = 1 - \exp(-U/E_D), \tag{6}$$

where U is the thermal energy of the compound nucleus, δW is the shell correction taken from the difference between the experimental and liquid drop model masses, E_D accounts for the rate at which the shell effect melts away with an increase of excitation energy, and $\tilde{a}$ is the asymptotic value to which the level density parameter approaches with increasing excitation energy of the compound nucleus. $\tilde{a}$ depends upon the nuclear mass and the shape in a fashion similar to the liquid drop model of mass [42].

We first perform statistical model calculation with $\beta = 0$ in Eq. (3) which reduces the Kramers' fission width to the Bohr-Wheeler transition state fission width corrected for the phase space due to vibrations around the ground state shape [12,43]. The calculated excitation functions for M^{pre} and M^{tot} are compared with the experimental values in Fig. 4. It is observed that pre-scission neutron multiplicities are underpredicted for all the cases though the total neutron multiplicities are reasonably well reproduced. This is due to the fact that emission of both pre- and post-scission neutrons together account for depletion of most of the initial excitation energy of the compound nucleus.

Pre-scission multiplicities are next calculated with different values of β in the Kramers' fission width. The fission width decreases with increasing values of β resulting in larger M^{pre} values. Figure 5 shows variation of M^{pre} values with β for different Rn isotopes at a number of given excitation

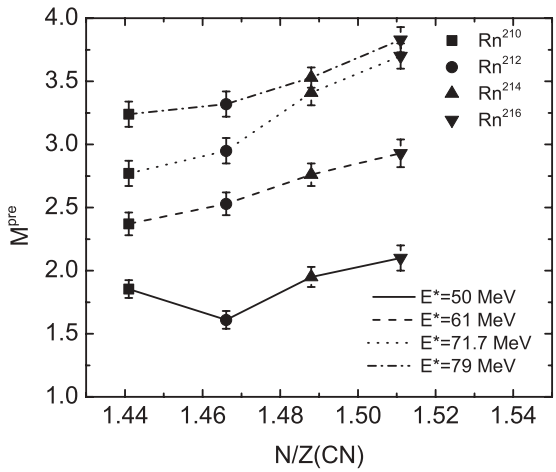

FIG. 3. Variation of M^{pre} with β for different systems. The experimental values are also shown.

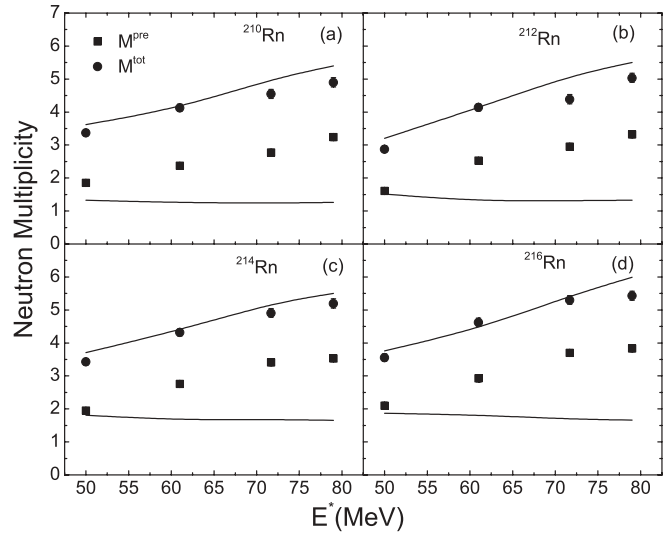

FIG. 4. (a)-(d) Experimental excitation functions of M^{pre} and M^{tot} with statistical model results for $\beta = 0$ (solid lines).

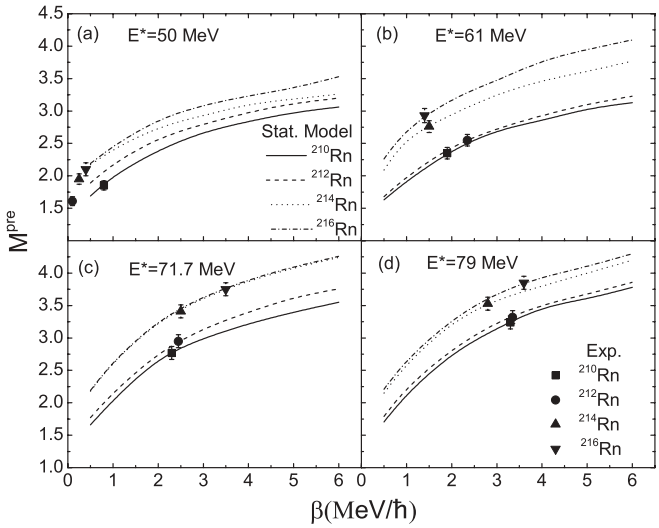

FIG. 5. (a)-(d) Variation of calculated $M^{\rm pre}$ with β for different systems. The experimental values are also shown. The value for which the calculated $M^{\rm pre}$ matches the experimental value is taken as the best-fit β value for a given system.

energies. The experimental $M^{\rm pre}$ values are also given in the plots. The value for which the calculated value of $M^{\rm pre}$ matches the experimental value is taken as the best-fit β value for a given system. The β dependences of $M^{\rm pre}$ in Fig. 5 are similar to those in Ref. [25]. However, the isotopic dependence of the present calculation is much weaker than that of Ref. [25] where calculations for systems with large N/Z variation are reported.

The best-fit β values at each excitation energy for each compound nucleus are given as a function of N/Z in Fig. 6. In this plot, the shaded area corresponds to the uncertainty in the fitted β values due to the experimental error in $M^{\rm pre}$. It is

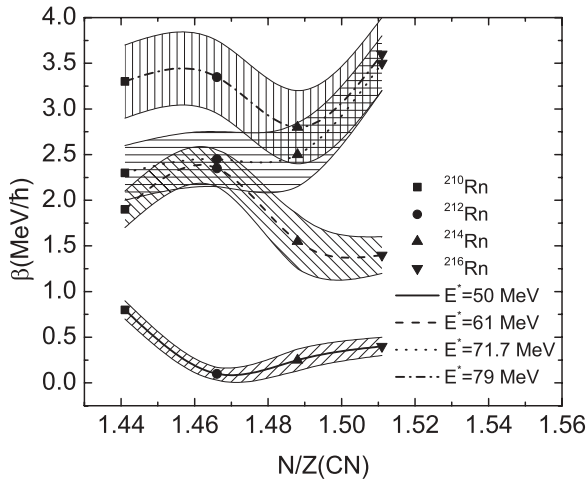

FIG. 6. Variation of the best-fit values of β with N/Z of the compound nuclei at different excitation energies. The shaded areas represent the uncertainty in β associated with the experimental error in $M^{\rm pre}$.

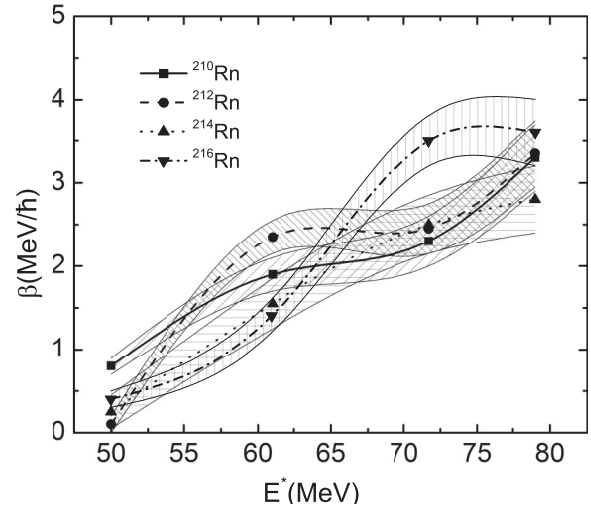

FIG. 7. Variation of the best-fit values of β with excitation energy for different compound nuclei. The shaded areas represent the uncertainty in β associated with the experimental error in $M^{\rm pre}$.

noted in this figure that the best-fit β has a minimum at ^{212}Rn for the lowest excitation energy, though at higher excitation energies, N/Z dependence of β does not show any specific trend. It is of further interest to note that the N/Z dependence of β is similar to the N/Z dependence of $M^{\rm pre}$ (Fig. 3) at the lowest excitation energy. Since the minimum in $M^{\rm pre}$ at ^{212}Rn cannot be understood in terms of neutron partial widths alone as we have discussed in the previous section, it indicates a shorter fission half-life for ^{212}Rn compared to the neighboring isotopes. Consequently, a minimum in β with respect to N/Z appears at ^{212}Rn. Since ^{212}Rn has a closed neutron shell at $N = 126$, the above N/Z dependence of β is also expected from the microscopic theory of one-body dissipation [44], where incoherent particle-hole excitations cause dissipation. In an isotopic chain with a closed shell nucleus, particle-hole excitation is easier for the nonclosed nuclei than the closed shell one, and consequently the former is expected to be more dissipative than the latter. Evidently, this picture is valid only at excitation energies where the shell structure persists. The present results thus suggest presence of shell effects at the lowest excitation energy. A similar observation is also made in a recent work [24] where measurements of pre-scission neutron multiplicities from Fr isotopes are reported. At higher excitation energies, however, the particle spectrum becomes more complex and the N/Z dependence of β does not present a clear picture.

The excitation energy dependence of the best-fit β values is shown in Fig. 7. We here observe a strong (initial) excitation energy dependence of β. Several factors not considered in the present study possibly contribute to the observed energy dependence. These include neglect of higher order terms in collective speed in the basic definition of the dissipative force [45] and shape dependence of dissipation [4]. It is, however, expected that the inclusion of the above effects will not alter the relative dissipation strengths of the nuclei at a given excitation energy.

V. SUMMARY AND CONCLUSION

Pre-scission neutron multiplicities have been measured for the ^{16,18}O + ^{194,198}Pt reactions forming compound nuclei at excitation energies of 50, 61, 71.7, and 79 MeV. The compound nuclei have the same value of Z but different neutron numbers. The measured pre-scission neutron multiplicities increases with the increase of N/Z of the compound nuclei at all excitation energies except the lowest one. Pre-scission multiplicities measured at the lowest excitation energy display a minimum at the compound nucleus ^{212}Rn with $N = 126$.

The measured multiplicities are analyzed with the statistical model of nuclear decay where fission hindrance due to nuclear dissipation is considered. The dissipation strength is treated as an adjustable parameter in order to fit the experimental data. The N/Z dependence of the dissipation strength at the lowest excitation energy of the compound nuclei suggests shell closure effects. However, such effects are not observed at higher excitations where the variation of the dissipation strength with N/Z does not show any specific trend.

ACKNOWLEDGMENTS

The authors would like to thank the accelerator groups (LINAC and Pelletron) of IUAC, New Delhi for providing beams of excellent quality throughout the experiment. The authors are grateful to Dr. A. Roy for his constant encouragement during the entire duration of the project. Comments and suggestions from Dr. S. Kailas is gratefully acknowledged. Help received from Mr. Abhilash, in making thin enriched ^{194}Pt target is acknowledged. Thanks are also due to Dr. S.K. Datta, Dr. S. Roy, Dr. B. P. Mohanty, Dr. Hardev Singh, R. P. Singh, P. Barua, M. Saxena, and M. Oswal for their help at various stages of the experiment and analysis. One of the authors (R.S.) would like to thank IUAC for providing support through a UFUP grant. B.R.B. acknowledges the Department of Atomic Energy (DAE), Government of India, for a DAE young scientist research grant (YSRA).

[1] D. Hilscher and H. Rossner, Ann. Phys. (Paris) **17**, 471 (1992).
[2] J. Cabrera, Th. Keutgen, Y. El Masri, Ch. Dufauquez, V. Roberfroid, I. Tilquin, J. Van Mol, R. Regimbart, R. J. Charity, J. B. Natowitz, K. Hagel, R. Wada, and D. J. Hinde, Phys. Rev. C **68**, 034613 (2003).
[3] J. P. Lestone, Phys. Rev. Lett. **70**, 2245 (1993).
[4] I. Diószegi, N. P. Shaw, I. Mazumdar, A. Hatzikoutelis, and P. Paul, Phys. Rev. C **61**, 024613 (2000).
[5] H. Rossner, D. Hilscher, D. J. Hinde, B. Gebauer, M. Lehmann, M. Wilpert, and E. Mordhorst, Phys. Rev. C **40**, 2629 (1989).
[6] D. J. Hinde, H. Ogata, M. Tanaka, T. Shimoda, N. Takahashi, A. Shinohara, S. Wakamatsu, K. Katori, and H. Okamura, Phys. Rev. C **39**, 2268 (1989).
[7] H. Rossner, D. J. Hinde, J. R. Leigh, J. P. Lestone, J. O. Newton, J. X. Wei, and S. Elfstrom, Phys. Rev. C **45**, 719 (1992).
[8] D. J. Hofman, B. B. Back, and P. Paul, Phys. Rev. C **51**, 2597 (1995).
[9] B. B. Back, D. J. Blumenthal, C. N. Davids, D. J. Henderson, R. Hermann, D. J. Hofman, C. L. Jiang, H. T. Penttila, and A. H. Wuosmaa, Phys. Rev. C **60**, 044602 (1999).
[10] C. R. Morton, D. J. Hinde, J. R. Leigh, J. P. Lestone, M. Dasgupta, J. C. Mein, J. O. Newton, and H. Timmers, Phys. Rev. C **52**, 243 (1995).
[11] H. A. Kramers, Physica (Amsterdam) **7**, 284 (1940).
[12] N. Bohr and J. A. Wheeler, Phys. Rev. **56**, 426 (1939).
[13] P. Grange and H. A. Weidenmüller, Phys. Lett. B **96**, 26 (1980).
[14] P. Grange, Li Jun-Qing, and H. A. Weidenmüller, Phys. Rev. C **27**, 2063 (1983).
[15] H. A. Weidenmüller and Zhang Jing-Shang, Phys. Rev. C **29**, 879 (1984).
[16] S. Hassani and P. Grange, Phys. Lett. B **137**, 281 (1984).
[17] H. Hofmann and J. R. Nix, Phys. Lett. B **122**, 117 (1983).
[18] A. Saxena, A. Chatterjee, R. K. Choudhury, S. S. Kapoor, and D. M. Nadkarni, Phys. Rev. C **49**, 932 (1994).
[19] V. S. Ramamurthy, S. S. Kapoor, R. K. Choudhury, A. Saxena, D. M. Nadkarni, A. K. Mohanty, B. K. Nayak, S. V. Sastry, S. Kailas, A. Chatterjee, P. Singh, and A. Navin, Phys. Rev. Lett. **65**, 25 (1990).
[20] A. C. Berriman, D. J. Hinde, M. Dasgupta, C. R. Morton, R. D. Butt, and J. O. Newton, Nature (London) **413**, 144 (2001).
[21] J. C. Pei, W. Nazarewicz, J. A. Sheikh, and A. K. Kerman, Phys. Rev. Lett. **102**, 192501 (2009).
[22] D. J. Hinde, R. J. Charity, G. S. Foote, J. R. Leigh, J. O. Newton, S. Ogazaza, and A. Chattejee, Nucl. Phys. A **452**, 550 (1986).
[23] J. O. Newton, D. J. Hinde, R. J. Charity, J. R. Leigh, J. J. M. Bokhorst, A. Chatterjee, G. S. Foote, and S. Ogaza, Nucl. Phys. A **483**, 126 (1988).
[24] Varinderjit Singh, B. R. Behera, Maninder Kaur, P. Sugathan, K. S. Golda, A. Jhingan, Jhilam Sadhukhan, Davinder Siwal, S. Goyal, S. Santra, A. Kumar, R. K. Bhowmik, M. B. Chatterjee, A. Saxena, Santanu Pal, and S. Kailas, Phys. Rev. C **86**, 014609 (2012).
[25] W. Ye, Eur. Phys. J. A **18**, 571 (2003).
[26] W. Ye, Phys. Rev. C **79**, 031601(R) (2009).
[27] S. Venkataramanan, Arti Gupta, K. S. Golda, Hardev Singh, Rakesh Kumar, R. P. Singh, and R. K. Bhowmik, Nucl. Instrum. Methods Phys. Res. A **596**, 248 (2008).
[28] R. A. Cecil, B. D. Anderson, and R. Madey, Nucl. Instrum. Methods **161**, 439 (1979).
[29] T. G. Masterson, Nucl. Instrum. Methods **88**, 61 (1970).
[30] D. Hilscher, J. R. Birkelund, A. D. Hoover, W. U. Schroder, W. W. Wilcke, J. R. Huizenga, A. C. Mignerey, K. L. Wolf, H. F. Breuer, and V. E. Viola, Phys. Rev. C **20**, 576 (1979).
[31] V. E. Viola, K. Kwiatkowski, and M. Walker, Phys. Rev. C **31**, 1550 (1985).
[32] K. J. Le Couteur and D. W. Lang, Nucl. Phys. **13**, 32 (1959).
[33] P. Fröbrich and I. I. Gontchar, Phys. Rep. **292**, 131 (1998).
[34] A. Bohr and B. R. Mottelson, *Nuclear Structure*, Vol. II, (Benjamin, London, 1975).
[35] E. G. Ryabov, A. V. Karpov, P. N. Nadtochy, and G. D. Adeev, Phys. Rev. C **78**, 044614 (2008).
[36] A. J. Sierk, Phys. Rev. C **33**, 2039 (1986).
[37] J. P. Lestone and S. G. McCalla, Phys. Rev. C **79**, 044611 (2009).
[38] K. H. Bhatt, P. Grange, and B. Hiller, Phys. Rev. C **33**, 954 (1986).

[39] Gargi Chaudhuri and Santanu Pal, Phys. Rev. C **65**, 054612 (2002).
[40] P. Grange, S. Hassani, H. A. Weidenmüller, A. Gavron, J. R. Nix, and A. J. Sierk, Phys. Rev. C **34**, 209 (1986).
[41] A. V. Ignatyuk, G. M. Smirenkin, and A. Tishin, Sov. J. Nucl. Phys. **21**, 255 (1975).
[42] W. Reisdorf, Z. Phys. A **300**, 227 (1981).
[43] V. M. Strutinsky, Phys. Lett. B **47**, 121 (1973).
[44] H. Hofmann and P. J. Siemens, Nucl. Phys. A **257**, 165 (1976).
[45] J. Blocki, Y. Boneh, J. R. Nix, J. Randrup, M. Robel, A. J. Sierk, and W. J. Swiatecki, Ann. Phys. (NY) **113**, 330 (1978).